Journal of Controlled Release 266 (2017) 301–309

Contents lists available at ScienceDirect

Journal of Controlled Release

journal homepage: www.elsevier.com/locate/jconrel

High-density lipoprotein mutant eye drops for the treatment of posterior eye diseases

Kenji Suda[a], Tatsuya Murakami[b,c,*], Norimoto Gotoh[a], Ryosuke Fukuda[b], Yasuhiko Hashida[c], Mitsuru Hashida[c,d], Akitaka Tsujikawa[a], Nagahisa Yoshimura[a]

[a] Department of Ophthalmology and Visual Sciences, Kyoto University Graduate School of Medicine, Kyoto, Japan
[b] Department of Biotechnology, Graduate School of Engineering, Toyama Prefectural University, Toyama, Japan
[c] Institute for Integrated Cell-Material Sciences, Kyoto University, Kyoto, Japan.
[d] Department of Drug Delivery Research, Graduate School of Pharmaceutical Sciences, Kyoto University, Kyoto, Japan

ARTICLE INFO

Keywords:
Ocular drug delivery
Age-related macular degeneration
Serum protein
Phospholipid, cell-penetrating peptide
Anti-angiogenesis drug

ABSTRACT

Age-related macular degeneration (AMD), in which choroidal neovascularization (CNV) affects the center of the retina (macula), leads to the irreversible visual loss. The intravitreal injection of anti-angiogenesis antibodies improved the prognosis of AMD, but relatively less invasive therapies should be explored. In the present study, we show that a high-density lipoprotein (HDL) mutant is a therapeutically active drug carrier capable of treating a posterior eye disease in mice via instillation. Various HDL mutants were prepared with apoA-I proteins fused with different cell-penetrating peptides (CPPs) and phospholipids with different alkyl chain lengths; their sizes were further controlled in the range of 10–25 nm. They were screened based on the efficiency of fluorescent dye delivery to the inner retinal layer in mice. The best mutant was found to have penetratin (PEN) as a CPP, 1,2-distearoyl-sn-glycero-3-phosphocholine (DSPC), and a size of 15 nm. In preclinical studies on a laser-induced CNV murine model, 1 week of instillation of the best mutant carrying the anti-angiogenesis drug pazopanib had dramatic therapeutic effects in reducing the CNV size. Importantly, the HDL mutant by itself contributed to the therapeutic effects. Future clinical trials for treating AMD with instillation of the HDL mutant are expected.

1. Introduction

Non-communicable diseases, that is, chronic non-infectious diseases of long duration, are increasingly widespread worldwide and are becoming some of the most serious health problems according to a United Nations High-Level Meeting in 2011 [1]. To combat these diseases, preemptive medicine, early interventions oriented to the individualized, and less invasive approaches are considered necessary [2]. Hopefully, novel nanotechnologies for disease-specific drug delivery systems (DDSs) as well as genomic approaches for understanding the underlying pathogeneses will play pivotal roles in achieving preemptive medicine [3].

In ophthalmologic fields, non-communicable disorders in the posterior segment of the eye are the main causes of social blindness: glaucoma, diabetic retinopathy, and age-related macular degeneration (AMD) [4]. Especially, AMD was one of the leading causes of blindness worldwide from 1990 to 2010, following cataract and glaucoma. The first option for AMD treatment nowadays is the intravitreal injection of anti-angiogenesis antibody [5,6]. This quite straightforward treatment has improved the prognosis of AMD [7], but in contrast, the social burden from the number of repeated injections [8] and the risk of sight-threatening complications such as endophthalmitis [9] have increased. Periocular injections such as subconjunctival and subtenon's may be other choices but cannot lessen these social burdens. Alternative therapies for eye injections, eye drops targeted the posterior segment of the eye, are developing [10], but none has proved to be effective in clinical practice [11,12].

Recent genome-wide association studies have indicated that the pathophysiology of AMD is based on the dysregulation of lipid metabolism, oxidative stress, and/or chronic inflammation [13,14]. Histological approaches also suggest that AMD especially shares a pathological mechanism with atherosclerosis [15] in terms of the existence of plaques with similar lipid and protein profiles and associations with macrophages. Thus, it is rational to hypothesize that preemptive therapies for atherosclerosis also have the potential to prevent or treat AMD.

High-density lipoprotein (HDL) has been drawing attention as a therapeutic target, especially to inhibit the onset of myocardial

* Corresponding author at: Department of Biotechnology, Graduate School of Engineering, Toyama Prefectural University, Toyama, Japan.
E-mail address: murakami@pu-toyama.ac.jp (T. Murakami).

http://dx.doi.org/10.1016/j.jconrel.2017.09.036
Received 16 June 2017; Received in revised form 19 September 2017; Accepted 27 September 2017
Available online 05 October 2017

infarction from atherosclerosis [16–18]. HDL has antiatherogenic properties arising from cholesterol efflux from the vascular endothelium and macrophages [19]. In fact, supplemental HDL therapies have been tested in many clinical trials [16]. Meanwhile, many experimental studies have reported on DDSs using reconstituted HDL nanoparticles [20,21] because of their high biocompatibility, relatively small sizes (approximately 10 nm), and hydrophobic cores. HDL can be reconstituted with phospholipids and recombinant apolipoprotein A-I (apoA-I) and thus are easily modified in various ways, i.e., by drug loading, genetic engineering, chemical modification, controlling lipid contents, and so on. Although modified HDL nanoparticles also hold great potential as formulations, their applications in the treatment of eye diseases have never been reported.

Our previous study revealed that genetic fusion of HDL with the TAT (Trans-Activator of Transcription) peptide, one of cell-penetrating peptides (CPPs), greatly improved intracellular drug delivery efficacy [22]. This property would be favorable for the better absorption of drugs by cells on the surface of the eye. Additionally, the smaller size of lipid nanoparticles would be advantageous for improved eye tissue penetration [23]. In addition to the antiatherogenic properties of HDL, these considerations motivated us to explore the potential of CPP-fused HDL nanoparticles as instillation formulations against AMD. In this study, we prepared various HDL mutants with different compositions and sizes and tested their therapeutic efficacy in a murine model of laser-induced choroidal neovascularization (CNV) and AMD.

2. Materials and methods

2.1. Materials

1,2-Dimyristoyl-sn-glycero-3-phosphocholine (DMPC), 1,2-dipalmitoyl-sn-glycero-3-phosphocholine (DPPC), and 1,2-distearoyl-sn-glycero-3-phosphocholine (DSPC) were obtained from NOF America Corporation (White Plains, NY, USA). Cholesterol, dicetyl phosphate (DCP), and coumarin-6 were obtained from Sigma-Aldrich (St. Louis, MI, USA). The Dc Protein Assay Kit was obtained from Bio-Rad Laboratories (Hercules, CA, USA). Spectra/Por Dialysis Membranes (molecular weight cut-off [MWCO], 3500 and 50,000) were obtained from Spectrum Laboratories (Rancho Dominguez, CA, USA). Fetal bovine serum (FBS) was obtained from Japan Bioserum (Hiroshima, Japan). Dulbecco's phosphate-buffered saline (pH 7.4, phosphate buffer saline (PBS)) and trypsin-EDTA (0.05% trypsin, 0.53 mM EDTA-4Na) were obtained from Invitrogen (Carlsbad, CA, USA). Cell culture dishes were obtained from BD Bioscience (San Jose, CA, USA). Dimethyl sulfoxide (DMSO) and potassium bromide (KBr) were purchased from Wako (Osaka, Japan). Pazopanib was purchased from SYNkinase (Parkville, Australia).

The expression vector pCold I was purchased from Takara Bio Inc. (Shiga, Japan). The *Escherichia coli* strain BL21(DE3) was obtained from Novagen (Madison, WI, USA). The Ni Sepharose resin was purchased from GE Healthcare (Buckinghamshire, UK). The restriction enzymes were purchased from TOYOBO (Osaka, Japan) and Takara Bio Inc. DNA polymerase and DNA ligase were purchased from Takara Bio Inc. Tryptone and yeast extract were obtained from BD (Franklin Lakes, NJ, USA). DH5-alpha, isopropyl beta-thiogalactopyranoside, and carbenicillin sodium salt were obtained from Wako.

2.2. Construction of cDNA for the expression of human apoA-I mutants

The construction of cDNA for the expression of human apoA-I mutants with or without a C-terminal TAT peptide was described previously [22]. Penetratin (PEN) and polyarginine (R8) peptide sequences (vide infra) were amplified with the following primers and inserted into the *Pst*I and *Xba*I sites of the pCOLD I bacterial expression vector for a similar C-terminal fusion. For fusion of these two CPPs with apoA-I, N-terminal 44 amino acid-deleted apoA-I cDNA, optimized for *E. coli* expression by Invitrogen, was used.

Forward primers: 5′-attctgcagcgccagattaaaatttggtttcagaaccgccgcatg-3′ (PEN), 5′-atctgcagcgccgccgccgccgccgccgctaatctagaaaactgctggataattggg-3′ (R8).

Reverse primers: 5′-attctagatttttttttccatttcatgcggcggttctgaaaccaaa-3′ (PEN), 5′-cccaattatccagcagttt-3′ (R8).

2.3. Preparation of human apoA-I mutants

All apoA-I mutants were expressed in BL21(DE3) according to the manufacturer's protocol and were purified on a Ni Sepharose column in an AKTA start chromatography system (GE Healthcare) under denaturation conditions. After dialysis against 0.4 mM hydrochloric acid at 4 °C with a Spectra/Por Dialysis Membrane (MWCO, 3500), proteins were lyophilized with an FDU-2200 lyophilizer (EYELA, Tokyo, Japan) and stored at − 80 °C until use.

2.4. Preparation of the HDL mutants and liposome

HDL mutants were prepared according to the procedure described by Jonas [24] with minor modifications. Briefly, phosphatidylcholine (PC; DMPC, DPPC, or DSPC) was solubilized in PBS containing 30 mg/mL sodium cholate, and mutated apoA-I protein was solubilized in PBS containing 4 M urea. These two solutions were mixed at the phase transition temperature (Tm) of each PC. Subsequently, for DMPC and DPPC, the mixture was incubated overnight at 24 °C and 41 °C, respectively. For DSPC, the mixture was incubated at 55 °C only for 30 min to reduce any side reactions. In all cases, the mixture was then dialyzed at room temperature (22 °C) overnight with a Spectra/Por Dialysis Membrane (MWCO, 50,000) to remove sodium cholate. The dialyzed solution was centrifuged at 16,500 × *g* at room temperature for 30 min to remove any debris. Thereafter, HDL samples were purified by density gradient ultracentrifugation according to the method by Kelley et al. with some modifications [25]. Briefly, the density of HDL samples (1 mL) was adjusted to 1.31 g/mL and layered beneath a four-step gradient (3.0 mL, 1.21 g/mL; 3.8 mL, 1.063 g/mL; 3.3 mL, 1.019 g/mL, 1.2 mL, 1.006 g/mL) in a polyallomer tube (Beckman Coulter Inc., Tokyo, Japan). Density adjustments were made with solid KBr. Ultracentrifugation was carried out at 24 °C in a Beckman Optima MAX-XP using an MLS50 rotor at 286,000 × *g*. The samples were collected from fractions in the 1.063–1.21 g/mL density range (see Fig. S3a, b).

For the preparation of small-size liposome (ssLip) formulations in our study, the procedure described by Hironaka et al. [26] was used with some modifications. Briefly, the lipid mixture of PC, DCP, and cholesterol and the cargo (coumarin-6 or pazopanib) at a molar ratio of 8:2:1:0.04 was dissolved in chloroform in a round-bottom flask and evaporated at 40 °C to form a thin lipid film using a rotary evaporator (EYELA). The film was freeze-dried overnight to completely remove chloroform. After adding PBS, the lipid film was sonicated at 65 °C for at least 10 min. The resulting suspension was passed through a polycarbonate membrane with pore size of 100 nm (Avanti Polar Lipids, Inc., Alabaster, AL, USA) in an Mini-Extruder (Avanti) at least 10 times.

2.5. Incorporation of coumarin-6 or pazopanib into HDL mutants

There are two timings for loading a drug or substance into the nascent HDL, which are before and after reconstitution of the HDL. For incorporation of coumarin-6, we used the former; coumarin-6 was mixed with PC in chloroform at a molar ratio of 8:0.04. Chloroform was evaporated at 40 °C using a rotary evaporator and then the residual lipid film was dried in vacuo overnight. The dried lipid film was solubilized in PBS containing 30 mg/mL sodium cholate and the following procedure was performed as described above. The amount of coumarin-6 was quantified with a FluoroMax-4 fluorometer (HORIBA, Kyoto, Japan) at an excitation wavelength of 490 nm and an emission

wavelength of 520 nm.

In contrast, the loading of pazopanib in a HDL mutant (HDL/PEN) was carried out by mixing HDL/PEN (750 μg on a protein basis) in PBS and pazopanib (100 μg) in DMSO at 55 °C for 1 h. The mixture was immediately purified by density gradient ultracentrifugation as described above. Pazopanib in HDL/PEN or ssLip was analyzed by the HPLC-UV method described by Escudero-Ortiz et al. [27] using an ACQUITY UPLC equipped with a BEH C18 column (Waters, Milford, MA, USA).

2.6. Evaluations of the HDL mutants and liposome

The amount of protein (apoA-I mutant) in the HDL mutants was determined via the Lowry method using a Dc Protein Assay Kit. The phospholipid in the HDL mutants or ssLip was quantified through a phospholipid-specific enzymatic assay using the Phospholipid C-test Wako (Wako Chemical Industries, Osaka, Japan). The hydrodynamic diameters and zeta potentials of the HDL mutants and ssLip were determined in PBS with a Nanotrac UPA-EX250 particle size analyzer (Nikkiso, Tokyo, Japan) and in 10% PBS with a Zetasizer Nano Z (Malvern, Worcestershire, UK), respectively.

The observation of the HDL mutants by transmission electron microscopy proceeded in accordance with the protocol described by Silva et al. [28]. In short, copper collodion film paste (400 mesh; Nisshin EM Co., Ltd., Tokyo, Japan) was floated for 20 s on a 15-μL droplet of the HDL mutant solution (2 μg/mL protein). Excess fluid was removed from the mesh. After washing with distilled water twice, the mesh with the absorbed the HDL mutants was floated on a 15-μL drop of uranyl acetate for 60 s. Excess stain was removed and the dried mesh was viewed at 80 KeV with a Hitachi H-7650 transmission electron microscope (Hitachi High-Technologies, Inc., Tokyo, Japan).

In the evaluation of the HDL mutants by atomic force microscopy (AFM), we used an HS-AFM apparatus (Research Institute of Biomolecule Metrology Co., Ltd. [RIBM], Tsukuba, Ibaraki, Japan). HDL samples in 2-μL PBS droplets (1 μg protein/mL) were adsorbed onto the mica substrate (RIBM) for 10 min after diluted with 10 μM phosphate buffer (pH 5.8). HDL samples were analyzed in solution by AC-mode AFM equipped with a NanoWorld USC-F1.2-k0.15 ultra-short cantilever (NanoWorld AG, Neuchâtel, Switzerland) at a scanning rate of 0.5 fps at 22 °C. To obtain the height and width data for the HDL particles, the scanning ranges were varied from 50 nm to 999 nm. The obtained AFM images were analyzed in Gwyddion (version 2.47; Department of Nanometrology, Czech Metrology Institute, Brno, Czech Republic), a free software package for SPM data analysis.

2.7. Mouse strains

All animals were handled in accordance with the Association for Research in Vision and Ophthalmology Statement for the Use of Animals in Ophthalmic and Vision Research and the Guideline for Animal Experiments of Kyoto University. All experimental procedures were approved by the Institutional Review Board of Kyoto University Graduate School of Medicine. All mice were maintained under a 12-h light/12-h dark cycle.

2.8. Evaluation of drug delivery efficiency to the posterior segment of the mouse eye

Awake male adult mice (C57BL6/J, SLC, Kyoto, Japan) weighing 20–30 g were used. A single dose of 3 μL of the sample was dropped onto the surface of the cornea using a micropipette. Since little coumarin-6 fluorescence was detected in the contralateral eye (Fig. S1), both eyes of three mice were treated with the samples under one experimental condition.

Except where otherwise indicated, the eyes were enucleated 30 min after topical administration and fixed in 4% paraformaldehyde (PFA) in PBS at 4 °C overnight, immersed in 20% sucrose at 4 °C for 24 h, and then embedded in OCT compound (Miles, Elkhart, IN, USA). Cryostat sections (14-μm thick) were mounted on Matsunami platinum-coated glass slides (Matsunami Glass, Osaka, Japan) and preserved at − 30 °C until evaluation by microscopy. Retinal images around the optic discs of frozen sections were observed by confocal microscopy (LSM 5 Pascal, Carl Zeiss, Tokyo, Japan) with fluorescence filters for FITC (emission: 488 nm, excitation: 506–530 nm). Within the area of the inner plexiform layer (IPL) at a distance between 100 and 200 μm from the optic disc, the fluorescence intensity of coumarin-6 was evaluated with ImageJ (version 1.50i; Wayne Rasband, National Institutes of Health, USA). The intensity data were obtained at six points from a single section (three sections per eye, six eyes from three mice) and a total of 108 values were averaged for the following analysis.

2.9. Pre-clinical studies in mice with laser-induced choroidal neovascularization (CNV)

The procedure for CNV induction was described previously [29]. Briefly, mice were anesthetized with 10 mg/kg of xylazine and 80 mg/kg of ketamine. Their pupils were fully dilated with 5% phenylephrine hydrochloride/0.8% tropicamide (Sandol P; Nitten, Nagoya, Japan). Cover glasses were positioned on their corneas for use as a contact lens. Laser photocoagulation was used to create CNV with four laser-induced burns in one eye four to five disc diameters away from the optic disc with the following settings: 75 μm, 0.05 s, and 150 mW (DC-3000, Nidek, Gamagori, Japan). Only burns with a bubble were included in this study since the formation of a bubble generally indicates a successful perforation of Bruch's membrane. Laser burns with any hemorrhage were excluded.

After the instillation of eye drops for 1 week twice a day, eyes with CNV were enucleated and fixed in 4% PFA in PBS for 20 min at 4 °C and sectioned at the limbus; the cornea, iris, and lens were discarded. For CNV quantification, RPE/choroidal flat mounts were stained according to previously described standard immunohistochemical procedures [30]. Rat anti-CD102 antibody (1:200, BD Pharmingen, San Diego, CA, USA) and Alexa 488-conjugated anti-rat IgG antibody (1:500, Invitrogen, Eugene, OR, USA) were used as the primary and secondary antibody, respectively. The RPE/choroidal complexes were laid flat and radial relaxing incisions were made to obtain a whole-mount preparation. Images were obtained by confocal microscopy (LSM 5 Pascal, Carl Zeiss, Tokyo, Japan).

2.10. Statistics

All values are reported as the mean ± standard error. A one-way analysis of variance (ANOVA) and post hoc Tukey correction were used to investigate differences in averages between more than two groups. All statistical analyses were performed using R ver. 3.1.2. $P < 0.05$ was considered statistically significant.

3. Results

3.1. Delivery of a fluorescent dye by a HDL mutant to the posterior eye segment

To test the feasibility of HDL mutants as eye drop drug carriers to the posterior segment of the eye, the first mutant was prepared with the TAT peptide and 1,2-dimyristoyl-sn-glycero-3-phosphocholine (DMPC) and loaded with a fluorescent cargo molecule (coumarin-6). This complex (DMPC-HDL/TAT) was administered to normal mice once through eye drop instillation. After 30 min, frozen sections of enucleated whole eyes were observed via confocal fluorescence microscopy, which enabled specific detection of coumarin-6 compared with epifluorescence microscopy frequently used in eye studies (Fig. 1A). The coumarin-6 fluorescence signal around the optic disc was clearly

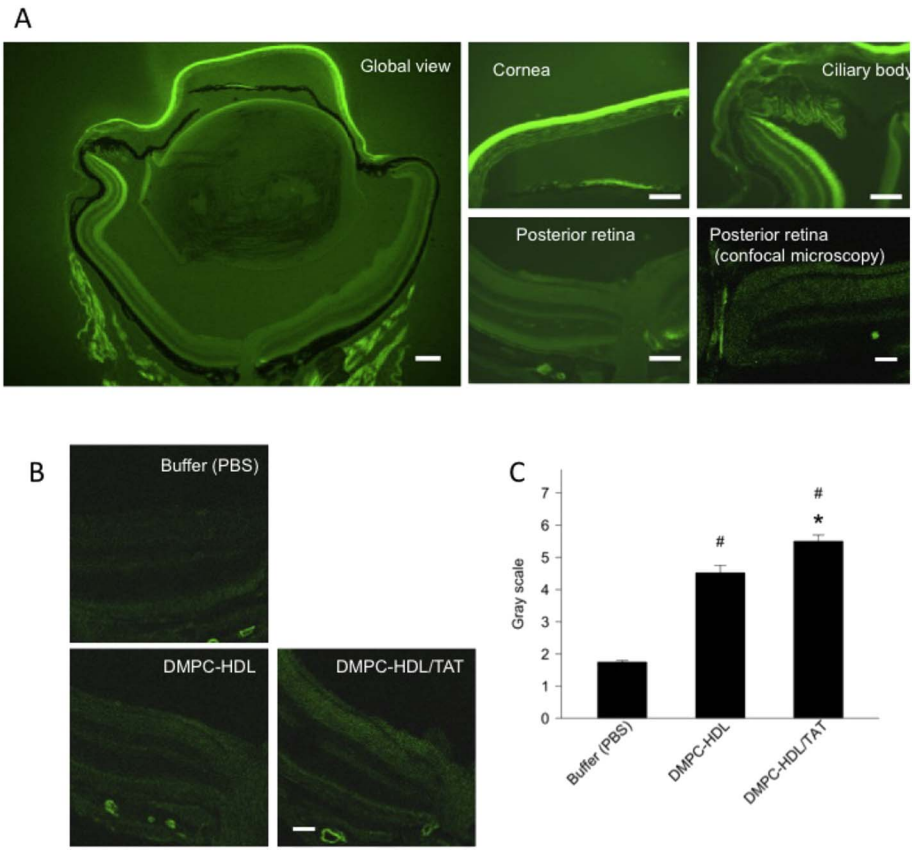

Fig. 1. Delivery of fluorescent cargo by using an HDL mutant to the posterior eye segment of a mouse via eye drop instillation. The cargo-loaded HDL mutant involves coumarin-6, the TAT peptide and DMPC (DMPC-HDL/TAT). Fluorescence images acquired 30 min after eye drop administration are shown. (A) Representative images of the entire eye, cornea, ciliary body, peripheral retina, posterior retina, and optic nerve are shown. Only the posterior retina and optic nerve have been analyzed via confocal microscopy. Scale bars, 200 μm in the global view; 50 μm in other focal views. (B) Representative confocal images of the posterior retina after topical administration of PBS, coumarin-6-loaded HDL composed of DMPC without CPP (DMPC-HDL), and DMPC-HDL/TAT. Scale bar, 50 μm. (C) A fluorescence intensity analysis of the inner layer of the posterior retina evaluated by grayscale. $\#p < 0.01$ compared with PBS. $*p < 0.05$ compared with HDL. Data are shown as the mean ± standard error.

detected, and the intensity was significantly higher than that of HDL without the TAT peptide (DMPC-HDL) (Fig. 1B, C), suggesting that upon eye drop instillation, HDL was able to deliver coumarin-6 to the posterior segment of the eye and the TAT peptide in HDL improved its delivery efficiency.

3.2. Optimization of the HDL mutant structure

These results encouraged us to optimize HDL mutants for better delivery to the posterior segment of the eye. Various coumarin-6-loaded HDL mutants with different CPPs and phospholipids were prepared and tested in the same manner. As a result, the best composite among those examined was found to be 1,2-distearoyl-sn-glycero-3-phosphocholine (DSPC) (Fig. 2A, B) and penetratin (PEN) (Fig. 2C, D). Differences in the phospholipid and CPP did not have a significant impact on the structural or physical properties of HDL mutants (Table S1, Figs. S2 and S3).

The sizes of drug carriers are also a key determinant of delivery efficiency. HDL mutants bearing DSPC and PEN with four different diameters ranging from 10 to 25 nm were carefully prepared by changing the protein/lipid molar ratio during HDL reconstitution (Fig. S4) and the best diameter among them was found to be 15 nm (Fig. 2E, F). This 15-nm HDL mutant bearing PEN and DSPC for eye drop instillation was designated HDL/PEN and used for further studies.

The time course of coumarin-6 delivery was evaluated 10–360 min after instillation. The coumarin-6 fluorescence intensity around the optic disc was maximal at 10 min and then monotonically decreased after that point. This profile was different from that of a small-sized liposome (ssLip) used as another lipidic eye drop formulation with a much larger diameter (Fig. 3).

3.3. Pre-clinical study of pazopanib-loaded HDL/PEN in a murine AMD model

Pre-clinical studies for HDL/PEN formulations were conducted in a murine model of AMD with pazopanib (Pzp), a tyrosine kinase inhibitor that was previously developed as a drug in an eye drop formulation including a beta-cyclodextrin derivative (Captisol; San Diego, CA, USA) for AMD (Fig. 4) [10]. The size and zeta potential (zeta) of Pzp-loaded HDL/PEN (Pzp@HDL/PEN) were nearly identical to those of the corresponding coumarin-6-loaded HDL/PEN (Table S2). One week after administration via instillation, the areas of laser-induced CNV were measured using confocal microscopy after immunofluorescent staining. Compared with sham treatment (PBS) and HDL/PEN alone, topical treatment with Pzp@HDL/PEN dramatically reduced the area of CNV (19,472.5 ± 1876.1 μm^2 in the PBS arm; 14,134.8 ± 938.3 μm^2 in the HDL/PEN arm; 9935.2 ± 602.5 μm^2 in the Pzp@HDL/PEN arm) (Fig. 4A, B). These results clearly demonstrate that Pzp@HDL/PEN has potent therapeutic efficacy in this murine AMD model and that HDL/PEN itself significantly contributes to the efficacy. More importantly, the average CNV areas in the Pzp@HDL/PEN arm were smaller than those with other eye drop formulations: Pzp solved in 8% Captisol (Pzp@Captisol) and Pzp-loaded ssLip (Pzp@ssLip) (16,436.3 ± 1875.1 μm^2 in the Captisol arm; 14,046.7 ± 1139.6 μm^2 in the ssLip arm) (Fig. 4C). No apparent damage to the cornea was detected after repeated eye drop instillation of Pzp@HDL/PEN (data not shown), and an in vitro assay of HDL/PEN in human corneal epithelium (HCE-T) cells showed no significant decrease in cell viability (Fig. 5). These results suggest that HDL/PEN is a therapeutically active eye drop drug carrier capable of safe and efficient drug delivery to the posterior segment of the eye.

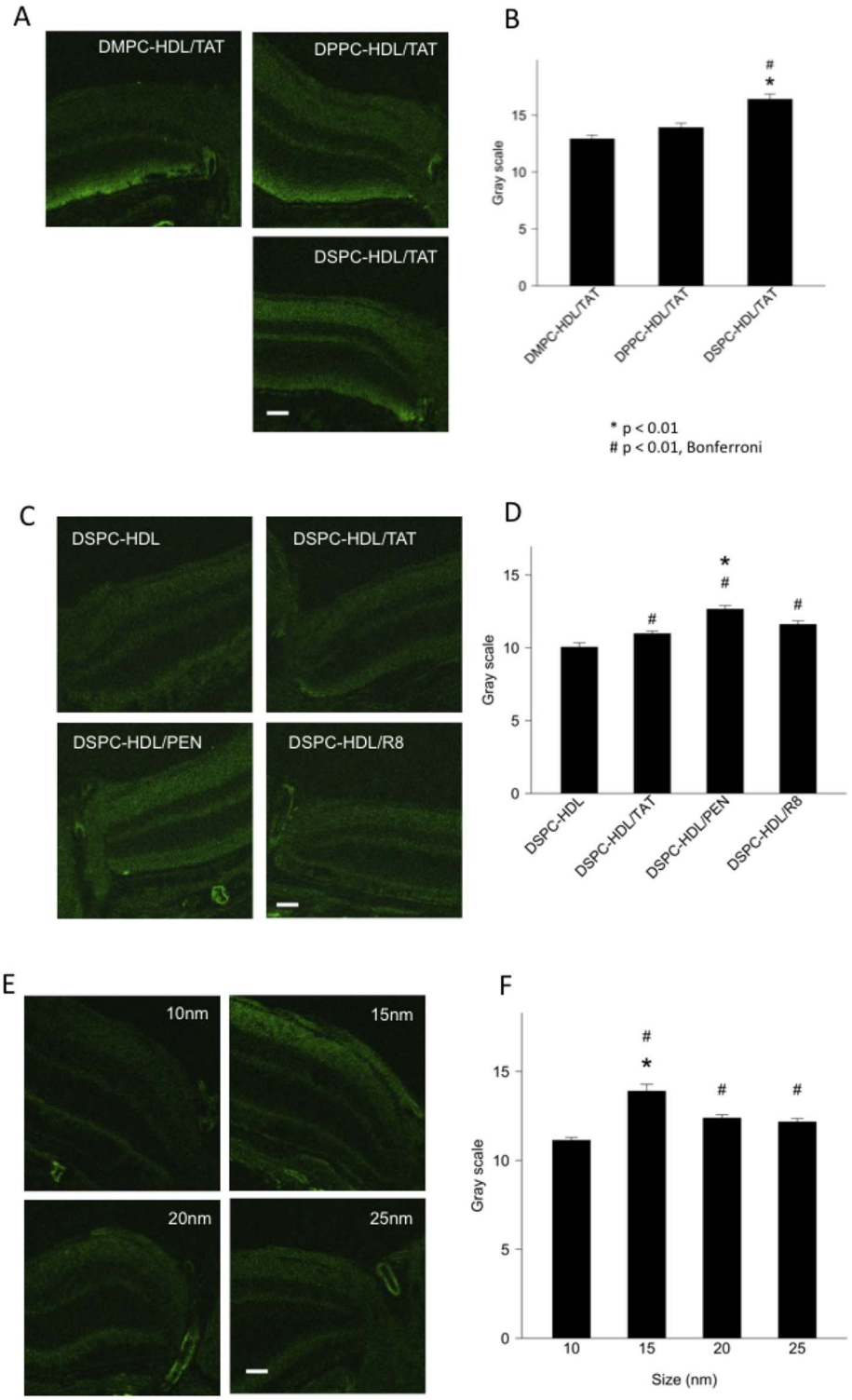

Fig. 2. Optimization of the HDL mutant structure. (A) Effect of the phospholipid structure. (B) A fluorescence intensity analysis of the inner layer of the posterior retina. $\#p < 0.01$ compared with the coumarin-6-loaded HDL mutant with DMPC (DMPC-HDL/TAT). $*p < 0.01$ compared with the coumarin-6-loaded HDL mutant with DPPC (DPPC-HDL/TAT). (C) Effect of the CPP structure. (D) A fluorescence intensity analysis of the inner layer of the posterior retina. $\#p < 0.05$ compared with coumarin-6-loaded HDL mutants with TAT (DSPC-HDL/TAT) or R8 (DSPC-HDL/R8). $*p < 0.05$ compared with the coumarin-6-loaded HDL mutant without CPP (DSPC-HDL). (E) Effect of HDL complex size. (F) A fluorescence intensity analysis of the inner layer of the posterior retina. $\#p < 0.05$ compared to the 10-nm HDL mutant complex. $*p < 0.05$ compared to the 20- and 25-nm HDL mutant complexes. Scale bar, 50 μm. Data are shown as the mean ± standard error.

3.4. Structural analyses of Pzp@HDL/PEN

The structural and physical characteristics of the HDL/PEN formulations prepared in this study are shown in Fig. 6, Fig. S2, and Table S1. HDL/PEN with Pzp at a ratio of 20 mM DSPC to 0.1 mM of apoA-I mutant with penetratin in PBS had a zeta of −8.6 mV and size of 17.8 nm in PBS. Transmission electron microscopy (TEM) micrographs of HDL/PEN with Pzp or coumarin-6 visualized nanoparticles approximately 20 nm in diameter (Fig. 6A, Fig. S3). Atomic force microscopy clearly showed that they were 15–30 nm in diameter and 4–6 nm in height (Fig. 6B–E), demonstrating that their shape was discoidal. Pzp@HDL/PEN had a larger diameter and height compared with the corresponding HDL prepared with DMPC (Fig. 6E, Fig. S5). Especially, the larger height is derived from DSPC's longer fatty acid chain (C18) than that of DMPC (C14). Circular dichroism (CD) analysis revealed that the protein moiety of HDL/PEN nanoparticles had a similar secondary structure to that of the parent HDL, irrespective of the type of CPP (Fig. 7).

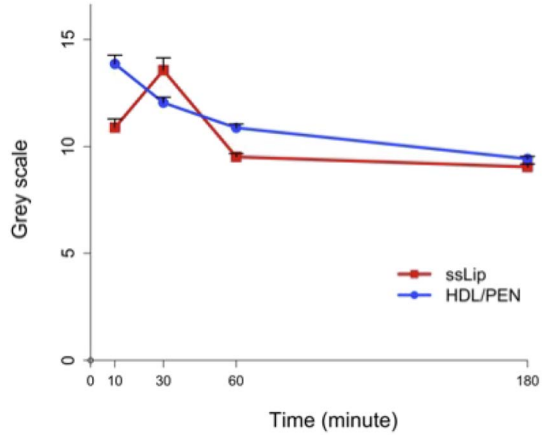

Fig. 3. A time course evaluation of coumarin-6 delivery using HDL/PEN or ssLip. Fluorescence intensity data at the inner layer of the posterior retina 10–360 min after instillation are shown. Data are shown as the mean ± standard error.

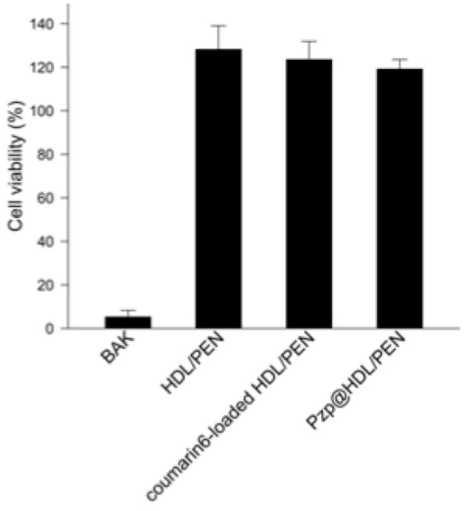

Fig. 5. Cytotoxicity of HDL/PEN with cultured corneal cells. Cell viability was evaluated after exposure to each sample for 3 h with cell counting kit-8. BAK: benzalkonium chloride in PBS. Data are shown as the mean ± standard error.

4. Discussion

Many researchers have evaluated HDLs as a supplemental therapy and have developed DDSs via oral, intravenous, and nasal routes of administration [31,32] since the last decade of the 20th century. The eye drop is the most common route of administration for the treatment of ocular diseases, but nevertheless, they have only been available for anterior segment eye diseases and rarely used for posterior segment diseases [33]. This is because there are several barriers (the cornea, conjunctiva, sclera, and blood-retinal barrier) to delivering drugs to the retina by eye drop instillation. Intravenously administered drugs also encounter the blood-retinal barrier before the retina. Thus, treatments for posterior segment eye diseases have been limited to the periocular

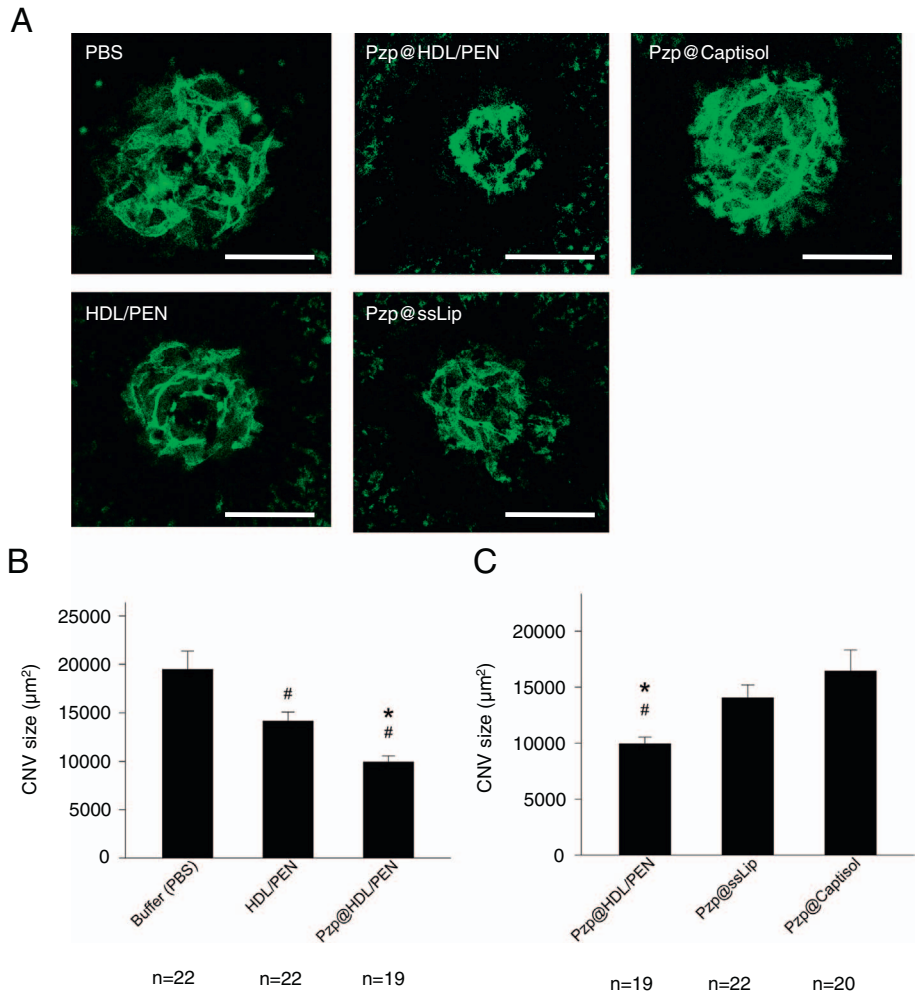

Fig. 4. A pre-clinical study of pazopanib (Pzp)-loaded HDL mutant in a murine AMD model. Mice with laser-induced CNV were used. (A) Confocal images of the CNV area stained with anti-ICAM2-antibody after 1 week of topical treatment with PBS, HDL mutant (HDL/PEN), or Pzp formulations containing HDL/PEN (Pzp@HDL/PEN), Captisol (β-cyclodextrin) (Pzp@Captisol), or a small-size liposome (Pzp@ssLip) are shown. Scale bar, 100 μm. (B) A comparison of CNV areas on confocal images 1 week after eye drop treatment of HDL/PEN without or with Pzp. #$p < 0.05$ compared with Buffer (PBS). *$p < 0.05$ compared with HDL/PEN (HDL mutant without Pzp). (C) A comparison of CNV areas on confocal images 1 week after eye drop treatment among three drug carriers. #$p < 0.05$ compared with Pzp@ssLip. *$p < 0.05$ compared with Pzp@Captisol. Data are shown as the mean ± standard error.

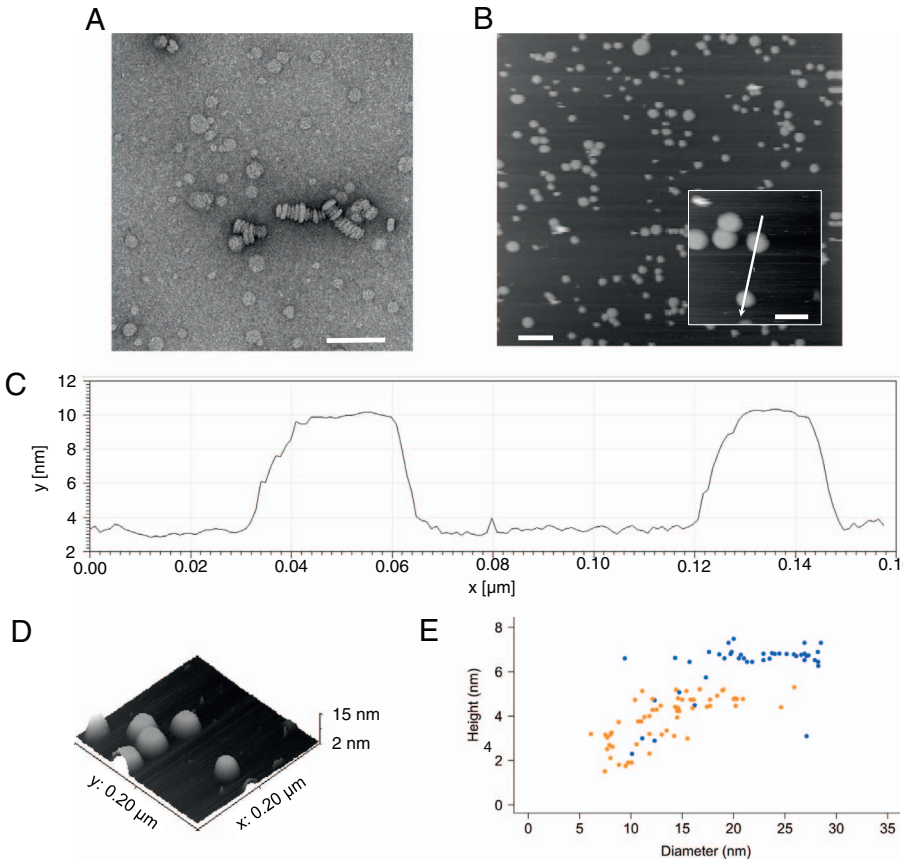

Fig. 6. Characteristics of Pzp@HDL/PEN. (A) A TEM image. Scale bar, 100 nm. (B) An AFM image in PBS. Scale bar, 100 nm. Inset, magnified images. Scale bar, 50 nm. (C) A sectional view from along the white arrow in the Fig. 6B inset. (D) A three-dimensional (3D) AFM image from the Fig. 6B inset. (E) A scatter plot of the diameters and heights of Pzp@HDL/PEN (blue) and its DMPC counterpart (orange) in PBS. (For interpretation of the references to colour in this figure legend, the reader is referred to the web version of this article.)

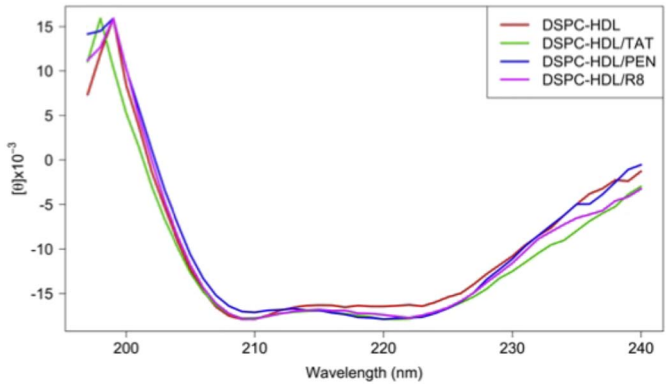

Fig. 7. Circular dichroism spectra of HDL and its mutants with DSPC in PBS.

or intravitreal injection of drugs. In this context, our preclinical study in a murine model of AMD revealed the beneficial therapeutic effect of HDL eye drops for the first time.

In nanotechnology applications for site-specific DDSs, the sizes of the drug carriers are one of the most important factors in controlling the pharmacokinetics and biodistribution of the drugs [34]. An important characteristic of reconstituted HDLs as a drug carrier is their small sizes. Inokuchi et al. reported on liposomes from 100 to 1000 nm and regarding the size for topical drug delivery to the posterior segment of the eye, stated that "the smaller, the better." [23] A similar size effect also has been observed for brain DDSs, in which nanoparticles 10–50 nm in diameter pass through the blood-brain barrier more easily than 100-nm diameter nanoparticles [35]. Whereas stable liposomes < 50 nm in diameter cannot be easily prepared, the size of reconstituted HDLs can be controlled in the range from approximately 9 to 40 nm simply by changing the phospholipid content [36]. On the other hand, studies on gold nanoparticles suggest that materials that are too small (< 5 nm) are easily washed out from target tissues [37]. In the context of these previous studies, our data on 15-nm HDL/PEN being the best size among the 10-, 15-, 20-, and 25-nm variants would result from the balance between the permeability of ocular tissues toward the posterior segment of the eye and residence stability.

The time course evaluation of the frozen sections revealed that coumarin-6 fluorescence intensity in the inner retinal layer decreased from 10 min after the instillation of HDL/PEN (Fig. 3), while the fluorescence intensity in the ssLip arm reached a maximum at 30 min after instillation and then declined faster than the HDL formulation. One of the reasons why the time courses were different between HDL/PEN and ssLip is the sizes of the particles, as discussed above. Generally, smaller particles can penetrate through barriers more rapidly. The slower rate of decline in the HDL/PEN arm may also result from some specific affinity of HDL/PEN to the posterior eye segment in mice since at least one of the HDL receptors, scavenger receptor BI, was reported to be expressed in the mouse retina [38]. Another reason may be the delivery route. Liposomes are considered to enter into the eye through tissues involved in the trabecular meshwork, iris, and ciliary body [26]. In contrast, after the instillation of fluorescently labeled HDL/PEN, the fluorescence intensity was higher in the cornea and conjunctiva compared to those in the iris and the ciliary body (Fig. 1). This distribution suggests putative (i) corneal-vitreal and (ii) conjunctival-scleral pathways. These two hypotheses are supported by previous studies of (i) CPP enhancing the absorption of a fluorescent dye bound to it through the cornea [39] and (ii) similar lipidic nanocarriers for triamcinolone acetonide having transscleral abilities [40]. To determine the precise pathway of delivery, further studies in larger species that are applicable to live imaging would be required. Additionally, detection of HDL/PEN or its components in the posterior eye segment would also be our next challenge.

The attachment of CPP to HDL yielded better coumarin-6 delivery

efficiency. This is caused by the prolonged retention of HDL/PEN on the negatively charged corneal surface, thereby leading to increased cell uptake [33]. In addition, our data suggest that the amount of the positive charge on CPP did not correlate with coumarin-6 delivery efficiency (Fig. 2C, D), which is in good agreement with the findings of the above-mentioned study showing that among four fluorescently labeled CPPs (TAT, PEN, polyarginine (R8), and protamine), PEN yielded the highest intensity fluorescence in the retina of the posterior segment of the eye in rats after eye drop instillation. In the same study, a strong negative band at 205 nm in the CD spectrum was suggested to be responsible for the greatest delivery efficiency of PEN [39], but was not obvious for HDL/PEN (Fig. 7). Nevertheless, the intrinsic physiological function of PEN in *Drosophila*, i.e., diffusion through the barriers of organs during development [41], might account for the deep penetration of HDL/PEN cargo into the ocular tissues in mice as well.

We found that DSPC was the best phospholipid for HDL mutant eye drops in terms of the ocular delivery of coumarin-6. This seems to be consistent with previous studies on ssLip [26]. Since DSPC has longer alkyl chains than other phospholipids (DMPC or 1,2-dipalmitoyl-sn-glycero-3-phosphocholine (DPPC)), the lipid bilayers of DSPC are more rigid because of its higher phase transition temperature, leading to the stabilization of nanoparticles. In fact, DSPC has been used for the preparation of solid lipid nanoparticles, which are promising drug carriers that can bind or incorporate various pharmaceutical agents and release them in a controlled manner [42].

One of the most striking findings of this study is that HDL/PEN itself has therapeutic effects on laser-induced CNV. In the fields of DDSs for inflammatory diseases and neoplasms, the paradigm of DDSs with intrinsic therapeutic effects is attracting attention and is termed “theralivery” [43]. Among the multiple therapeutic effects of HDL [44], reverse cholesterol transport can directly counteract atherogenesis, which is characterized by an accumulation of excess cholesterol and oxidized lipids from macrophages in the arterial wall. These abnormalities cause various inflammatory responses mediated by macrophages [45]. HDL also inhibits chronic inflammation directly through interaction with ATP-binding cassette transporter A1, scavenger receptor type I, and the sphingosine-1-phosphate receptors of macrophages via intracellular signaling pathway to inhibition of NF-κB. Moreover, genome-wide association studies indicate that the onset of clinical AMD is associated with lipid metabolism dysfunction followed by oxidative stress and chronic inflammation, which are the very pathogeneses targeted by HDL, as shown above. The mechanism by which HDL/PEN itself has therapeutic effects on mice with laser-induced CNV remains uncertain because its pathogenesis, i.e., acute inflammation after traumatic injury induced by laser ablation, is quite different from that of native AMD. Nevertheless, HDL/PEN may also provide therapeutic benefits in clinical AMD because its pathogenetic factors are all counteracted by HDL.

5. Conclusions

We have developed a new serum protein-based eye drop. Reconstituted HDL is a therapeutically active eye drop against AMD model mice and its genetic engineering to increase the cytophilicity is an effective strategy to improve the drug delivery efficiency to the posterior segment of the mouse eye. The alkyl chain length of phospholipids and size of a genetically engineered HDL are another factors for controlling the efficiency. Given that the design and preparation procedure of the best mutant (HDL/PEN) are simple, future clinical trials for treating age-related retinal diseases by its instillation are highly expected.

Funding

This study was supported in part by the World Premier International Research Center Initiative (WPI), the Ministry of Education, Culture, Sports, Science, & Technology (MEXT), Japan, and Grant-in-Aids for Scientific Research (no. 26670754 [N.G.] and no. 16H06909 [K.S.]), the Japan Society for the Promotion of Science (JSPS), Japan, Kyoto City (K.S., T.M.), Suzuken Memorial Foundation (T.M.), and CASIO Science Promotion Foundation (T.M.).

Author contributions

K.S. designed and performed the experiments, analyzed the data, and wrote the paper; T.M. conceived of and developed eye drop drug delivery system strategies using HDL, designed the experiments, and wrote the paper; N.G. conceived of and developed the strategies; R.F. designed and performed the experiments; Y.H. and M.H. designed and performed the circular dichroism analysis experiments; and A.T. and N.Y. supervised the project.

Competing interests

N.Y. is a paid advisory board member for NIDEK CO., LTD., and is a paid advisory board member for Topcon Corporation, outside the submitted work. We have applied the technology of drug delivery system in this paper for a patent (PCT/JP2015/086203) and are preparing to transfer it into the nation phase in other countries.

Acknowledgments

We thank the Center for Anatomical, Pathological, and Forensic Medical Research Graduate School of Medicine, Kyoto University for technical assistance in transmission electron microscopy observation, and the Research Institute of Biomolecule Metrology Co., Ltd. for performing atomic force microscopy.

Appendix A. Supplementary data

Supplementary data to this article can be found online at https://doi.org/10.1016/j.jconrel.2017.09.036.

References

[1] Political declaration of the High-level Meeting of the General Assembly on the Prevention and Control of Non-communicable Diseases. World Health Organization, New York City, NY, 16 September 2011. Available from URL: http://www.who.int/nmh/events/un_ncd_summit2011/political_declaration_en.pdf.
[2] H. Imura, Life course health care and preemptive approach to non-communicable diseases, Proc. Jpn Acad. Ser. B 89 (2013) 462–473.
[3] P. Couvreur, C. Vauthier, Nanotechnology: intelligent design to treat complex disease, Pharm. Res. 23 (2006) 1417–1450.
[4] R.R.A. Bourne, G.A. Stevens, R.A. White, J.L. Smith, S.R. Flaxman, H. Price, J.B. Jonas, J. Keeffe, J. Leasher, K. Naidoo, K. Pesudovs, S. Resnikoff, H.R. Taylor, Causes of vision loss worldwide, 1990–2010: a systematic analysis, Lancet Glob. Health 1 (2013) 339–349.
[5] N. Ferrara, L. Damico, N. Shams, H. Lowman, R. Kim, Development of ranibizumab, an anti-vascular endothelial growth factor antigen binding fragment, as therapy for neovascular age-related macular degeneration, Retina 26 (2006) 859–870.
[6] J.S. Heier, D.M. Brown, V. Chong, J.F. Korobelnik, P.K. Kaiser, Q.D. Nguyen, B. Kirchhof, A. Ho, Y. Ogura, G.D. Yancopoulos, N. Stahl, R. Vitti, A.J. Berliner, Y. Soo, M. Anderesi, G. Groetzbach, B. Sommerauer, R. Sandbrink, C. Simader, U. Schmidt-Erfurth, Intravitreal aflibercept (VEGF trap-eye) in wet age-related macular degeneration, Ophthalmology 119 (2012) 2537–2548.
[7] S. Rofagha, R.B. Bhisitkul, D.S. Boyer, S.R. Sadda, K. Zhang, Seven-year outcomes in ranibizumab-treated patients in ANCHOR, MARINA, and HORIZON: a multicenter cohort study (SEVEN-UP), Ophthalmology 120 (2013) 2292–2299.
[8] G.A. Lalwani, P.J. Rosenfeld, A.E. Fung, S.R. Dubovy, S. Michels, W. Feuer, J.L. Davis, H.W. Flynn, M. Esquiabro, A variable-dosing regimen with intravitreal ranibizumab for neovascular age-related macular degeneration: year 2 of the PrONTO Study, Am J. Ophthalmol. 148 (2009) 43–58.e1.
[9] S. Day, K. Acquah, P. Mruthyunjaya, D.S. Grossman, P.P. Lee, F.A. Sloan, Ocular complications after antivascular endothelial growth factor therapy in medicare patients with age-related macular degeneration, Am J. Ophthalmol. 152 (2011) 266–272.
[10] Y. Yafai, X.M. Yang, M. Niemeyer, A. Nishiwaki, J. Lange, P. Wiedemann, A.G. King, T. Yasukawa, W. Eichler, Anti-angiogenic effects of the receptor tyrosine kinase inhibitor, pazopanib, on choroidal neovascularization in rats, Eur. J. Pharmacol. 666 (2011) 12–18.

[11] K.G. Csaky, P.U. Dugel, A.J. Pierce, M.A. Fries, D.S. Kelly, R.P. Danis, J.I. Wurzelmann, C.F. Xu, M. Hossain, T. Trivedi, Clinical evaluation of pazopanib eye drops versus ranibizumab intravitreal injections in subjects with neovascular age-related macular degeneration, Ophthalmology 122 (2015) 579–588.
[12] R. Danis, M.M. McLaughlin, M. Tolentino, G. Staurenghi, L. Ye, C.-F. Xu, R.Y. Kim, M.W. Johnson, Pazopanib eye drops: a randomised trial in neovascular age-related macular degeneration, Br. J. Ophthalmol. (2013) 172–178.
[13] L.G. Fritsche, W. Chen, M. Schu, B.L. Yaspan, Y. Yu, G. Thorleifsson, D.J. Zack, S. Arakawa, V. Cipriani, S. Ripke, R.P. Igo, G.H.S. Buitendijk, X. Sim, D.E. Weeks, R.H. Guymer, J.E. Merriam, P.J. Francis, G. Hannum, A. Agarwal, A.M. Armbrecht, I. Audo, T. Aung, G.R. Barile, M. Benchaboune, A.C. Bird, P.N. Bishop, K.E. Branham, M. Brooks, A.J. Brucker, W.H. Cade, M.S. Cain, P.A. Campochiaro, C.-C. Chan, C.-Y. Cheng, E.Y. Chew, K.A. Chin, I. Chowers, D.G. Clayton, R. Cojocaru, Y.P. Conley, B.K. Cornes, M.J. Daly, B. Dhillon, A.O. Edwards, E. Evangelou, J. Fagerness, H.A. Ferreyra, J.S. Friedman, A. Geirsdottir, R.J. George, C. Gieger, N. Gupta, S.A. Hagstrom, S.P. Harding, C. Haritoglou, J.R. Heckenlively, F.G. Holz, G. Hughes, J.P.A. Ioannidis, T. Ishibashi, P. Joseph, G. Jun, Y. Kamatani, N. Katsanis, C.N. Keilhauer, J.C. Khan, I.K. Kim, Y. Kiyohara, B.E.K. Klein, R. Klein, J.L. Kovach, I. Kozak, C.J. Lee, K.E. Lee, P. Lichtner, A.J. Lotery, T. Meitinger, P. Mitchell, S. Mohand-Saïd, A.T. Moore, D.J. Morgan, M.A. Morrison, C.E. Myers, A.C. Naj, Y. Nakamura, Y. Okada, A. Orlin, M.C. Ortube, M.I. Othman, C. Pappas, K.H. Park, G.J.T. Pauer, N.S. Peachey, O. Poch, R.R. Priya, R. Reynolds, A.J. Richardson, R. Ripp, G. Rudolph, E. Ryu, J.-A. Sahel, D.A. Schaumberg, H.P.N. Scholl, S.G. Schwartz, W.K. Scott, H. Shahid, H. Sigurdsson, G. Silvestri, T.A. Sivakumaran, R.T. Smith, L. Sobrin, E.H. Souied, D.E. Stambolian, H. Stefansson, G.M. Sturgill-Short, A. Takahashi, N. Tosakulwong, B.J. Truitt, E.E. Tsironi, A.G. Uitterlinden, C.M. van Duijn, L. Vijaya, J.R. Vingerling, E.N. Vithana, A.R. Webster, H.-E. Wichmann, T.W. Winkler, T.Y. Wong, A.F. Wright, D. Zelenika, M. Zhang, L. Zhao, K. Zhang, M.L. Klein, G.S. Hageman, G.M. Lathrop, K. Stefansson, R. Allikmets, P.N. Baird, M.B. Gorin, J.J. Wang, C.C.W. Klaver, J.M. Seddon, M.A. Pericak-Vance, S.K. Iyengar, J.R.W. Yates, A. Swaroop, B.H.F. Weber, M. Kubo, M.M. Deangelis, T. Léveillard, U. Thorsteinsdottir, J.L. Haines, L.A. Farrer, I.M. Heid, G.R. Abecasis, Seven new loci associated with age-related macular degeneration, Nat. Genet. 45 (2013) 433–439 (439e1–2).
[14] I.A. Pikuleva, C.A. Curcio, Cholesterol in the retina: the best is yet to come, Prog. Retin. Eye Res. 41 (2014) 64–89.
[15] C.A. Curcio, M. Johnson, J.-D. Huang, M. Rudolf, Apolipoprotein B-containing lipoproteins in retinal aging and age-related macular degeneration, J. Lipid Res. 51 (2010) 451–467.
[16] B.A. Kingwell, M.J. Chapman, A. Kontush, N.E. Miller, HDL-targeted therapies: progress, failures and future, Nat. Rev. Drug Discov. 13 (2014) 445–464.
[17] T. Gordon, W.P. Castelli, M.C. Hjortland, W.B. Kannel, T.R. Dawber, High density lipoprotein as a protective factor against coronary heart disease, Am. J. Med. 62 (1977) 707–714.
[18] G.J. Miller, N.E. Miller, Plasma-high-density-lipoprotein concentration and development of ischæmic heart-disease, Lancet 305 (1975) 16–19.
[19] A. Rohatgi, A. Khera, J.D. Berry, E.G. Givens, C.R. Ayers, K.E. Wedin, I.J. Neeland, I.S. Yuhanna, D.R. Rader, J.A. de Lemos, P.W. Shaul, HDL cholesterol efflux capacity and incident cardiovascular events, N. Engl. J. Med. 371 (2014) 2383–2393.
[20] D. Schouten, M. van der Kooij, J. Muller, M.N. Pieters, M.K. Bijsterbosch, T.J. van Berkel, Development of lipoprotein-like lipid particles for drug targeting: neo-high density lipoproteins, Mol. Pharmacol. 44 (1993) 486–492.
[21] D.A. Bricarello, J.T. Smilowitz, A.M. Zivkovic, J.B. German, A.N. Parikh, Reconstituted lipoprotein: a versatile class of biologically-inspired nanostructures, ACS Nano 5 (2011) 42–57.
[22] T. Murakami, W. Wijagkanalan, M. Hashida, K. Tsuchida, Intracellular drug delivery by genetically engineered high-density lipoprotein nanoparticles, Nanomedicine (London) 5 (2010) 867–879.
[23] Y. Inokuchi, K. Hironaka, T. Fujisawa, Y. Tozuka, K. Tsuruma, M. Shimazawa, H. Takeuchi, H. Hara, Physicochemical properties affecting retinal drug/coumarin-6 delivery from nanocarrier systems via eyedrop administration, Investig. Ophthalmol. Vis. Sci. 51 (2010) 3162–3170.
[24] A. Jonas, Reconstitution of high-density lipoproteins, Methods Enzymol. 128 (1986) 553–582.
[25] J.L. Kelley, A.W. Kruski, Density gradient ultracentrifugation of serum lipoproteins in a swinging bucket rotor, Methods Enzymol. 128 (1986) 170–181.
[26] K. Hironaka, Y. Inokuchi, Y. Tozuka, M. Shimazawa, H. Hara, H. Takeuchi, Design and evaluation of a liposomal delivery system targeting the posterior segment of the eye, J. Control. Release 136 (2009) 247–253.
[27] V. Escudero-Ortiz, J.J. Pérez-Ruixo, B. Valenzuela, Development and validation of an HPLC-UV method for pazopanib quantification in human plasma and application to patients with cancer in routine clinical practice, Ther. Drug Monit. 37 (2015) 172–179.
[28] R.A.G.D. Silva, R. Huang, J. Morris, J. Fang, E.O. Gracheva, G. Ren, A. Kontush, W.G. Jerome, K.-A. Rye, W.S. Davidson, Structure of apolipoprotein A-I in spherical high density lipoproteins of different sizes, Proc. Natl. Acad. Sci. U. S. A. 105 (2008) 12176–12181.
[29] K. Suda, C. Guo, A. Oishi, S. Ikeda, A. Uemura, N. Yoshimura, Therapeutic potential of semaphorin 3E for the treatment of choroidal neovascularization, Investig. Ophthalmol. Vis. Sci. 55 (2014) 4700–4706.
[30] C. Campa, I. Kasman, W. Ye, W.P. Lee, G. Fuh, N. Ferrara, Effects of an anti-VEGF-A monoclonal antibody on laser-induced choroidal neovascularization in mice: optimizing methods to quantify vascular changes, Investig. Ophthalmol. Vis. Sci. 49 (2008) 1178–1183.
[31] M. Navab, G.M. Anantharamaiah, S.T. Reddy, S. Hama, G. Hough, V.R. Grijalva, N. Yu, B.J. Ansell, G. Datta, D.W. Garber, A.M. Fogelman, Apolipoprotein A-I mimetic peptides - ATVB in focus, Arterioscler. Thromb. Vasc. Biol. 25 (2005) 1325–1331.
[32] M. Huang, M. Hu, Q. Song, H. Song, J. Huang, X. Gu, X. Wang, J. Chen, T. Kang, X. Feng, D. Jiang, G. Zheng, H. Chen, X. Gao, GM1-modified lipoprotein-like nanoparticle: multifunctional nanoplatform for the combination therapy of Alzheimer's disease, ACS Nano 9 (2015) 10801–10816.
[33] R. Gaudana, J. Jwala, S.H.S. Boddu, A.K. Mitra, Recent perspectives in ocular drug delivery, Pharm. Res. 26 (2009) 1197–1216.
[34] D.H. Jo, J.H. Kim, T.G. Lee, J.H. Kim, Size, surface charge, and shape determine therapeutic effects of nanoparticles on brain and retinal diseases, Nanomedicine 11 (2015) 1603–1611.
[35] W.H. De Jong, W.I. Hagens, P. Krystek, M.C. Burger, A.J.A.M. Sips, R.E. Geertsma, Particle size-dependent organ distribution of gold nanoparticles after intravenous administration, Biomaterials 29 (2008) 1912–1919.
[36] J.B. Massey, H.J. Pownall, Cholesterol is a determinant of the structures of discoidal high density lipoproteins formed by the solubilization of phospholipid membranes by apolipoprotein A-I, Biochim. Biophys. Acta 1781 (2008) 245–253.
[37] R.K. Jain, T. Stylianopoulos, Delivering nanomedicine to solid tumors, Nat. Rev. Clin. Oncol. 7 (2010) 653–664.
[38] K.G. Duncan, K. Hosseini, K.R. Bailey, H. Yang, R.J. Lowe, M.T. Matthes, J.P. Kane, M.M. LaVail, D.M. Schwartz, J.L. Duncan, Expression of reverse cholesterol transport proteins ATP-binding cassette A1 (ABCA1) and scavenger receptor BI (SR-BI) in the retina and retinal pigment epithelium, Br. J. Ophthalmol. 93 (2009) 1116–1120.
[39] C. Liu, L. Tai, W. Zhang, G. Wei, W. Pan, W. Lu, Penetratin, a potentially powerful absorption enhancer for noninvasive intraocular drug delivery, Mol. Pharm. 11 (2014) 1218–1227.
[40] J. Araujo, S. Nikolic, M.A. Egea, E.B. Souto, M.L. Garcia, Nanostructured lipid carriers for triamcinolone acetonide delivery to the posterior segment of the eye, Colloids Surf. B: Biointerfaces 88 (2011) 150–157.
[41] M. Lindgren, U. Langel, Cell-penetrating Peptides - Methods and Protocols, second ed, Humana Press, New York, 2015.
[42] M.B. De Jesus, I.S. Zuhorn, Solid lipid nanoparticles as nucleic acid delivery system: properties and molecular mechanisms, J. Control. Release 201 (2015) 1–13.
[43] R. Kannan Mutharasan, L. Foit, C. Shad Thaxton, High-density lipoproteins for therapeutic delivery systems, J. Mater. Chem. B 4 (2016) 188–197.
[44] A. von Eckardstein, D. Kardassis, High Density Lipoproteins: From Biological Understanding to Clinical Exploitation, Springer International Publishing, Cham, 2015.
[45] P.P. Toth, P.J. Barter, R.S. Rosenson, W.E. Boden, M.J. Chapman, M. Cuchel, R.B. D'Agostino, M.H. Davidson, W.S. Davidson, J.W. Heinecke, R.H. Karas, A. Kontush, R.M. Krauss, M. Miller, D.J. Rader, High-density lipoproteins: a consensus statement from the National Lipid Association, J. Clin. Lipidol. 7 (2013) 484–525.